10. Kazakova KS, Yeroshenko GA, Sheshukova OV, Trufanova VP, Polishchuk TV, Maksymenko AI, et al. Dynamics of expression of carbohydrate determinants of fucosespecific lectin of the bark of golden rain in the mucosa of the attached part of the gums of rats under chronic ethanol intoxication. World of Medicine and Biology. 2023;85(3):216–218. DOI: 10.26724/2079-8334-2023-3-85-216-219.
11. Levkiv M, Patskan L, Pohoretska K, Manashchuk N, Zaliznyak M, Tverdokhlib N. Comparative analysis of dysbiotic changes in the oral cavity of patients with periodontal diseases and systemic pathologies. Explor Med. 2024;5:574–583. DOI: 10.37349/emed.2024.00241.

Стаття надійшла 9.08.2024 р.

DOI 10.26724/2079-8334-2025-3-93-171-176
UDC 611.831.7

G.E. Kerimzade
Azerbaijan Medical University, Baku, Azerbaijan

AGE-RELATED MORPHOLOGICAL FEATURES OF THE INTRACRANIAL (CISTERNAL) SEGMENT OF THE FACIAL NERVE DURING THE POSTNATAL PERIOD

e-mail: kerimzade73@list.ru

The study of the intratruncal structure of the facial nerve has long been a focus of interest for researchers. In this article, the age-related morphological features of the facial nerve segment extending from the base of the brain to the internal acoustic meatus were examined. The material consisted of cross-sections of the intracranial (cisternal) portion of the facial nerve, obtained from 96 human cadavers of both sexes and various stages of postnatal development. According to the case history, no pathological changes were identified in the skull or temporal bone, and no facial nerve pathologies were recorded in any of the cadavers. For histological examination, the cadavers from which the study material was obtained were divided into five age groups: group I (7–12 years) – 8 cadavers; group II (13–20 years) – 11 cadavers, group III (21–35 years) – 22 cadavers, group IV (36–57 years) – 35 cadavers and group V (58–74 years) – 20 cadavers. The samples were fixed in a solution containing 2 % paraformaldehyde, 2 % glutaraldehyde, and 0.1 % picric acid in 0.1 M phosphate buffer (pH 7.4). The results showed that in adults, the shape of the facial nerve is either oval or irregular, but its configuration is not directly related to the internal organization of the nerve. The number and arrangement of nerve bundles, as well as their myeloarchitectonic structure, are determined by the characteristics of early ontogeny. The study also found that the shape, size, number, and topography of the nerve bundles are variable parameters that depend on both individual features and age. These indicators are closely related to the connective tissue stroma of the nerve trunk.

Key words: facial nerve, myeloarchitectonics, myelinated nerve fibers, connective tissue stroma.

Г.Е. Керімзаде

ВІКОВІ МОРФОЛОГІЧНІ ОСОБЛИВОСТІ ВНУТРІШНЬОЧЕРЕПНОГО (ЦИСТЕРНАЛЬНОГО) СЕГМЕНТУ ЛИЦЕВОГО НЕРВА У ПОСТНАТАЛЬНОМУ ПЕРІОДІ

Вивчення внутрішньоствольної структури лицевого нерва тривалий час перебувало у центрі уваги дослідників. У цьому дослідженні розглядалися вікові морфологічні особливості сегмента лицевого нерва, що тягнеться від основи мозку до внутрішнього слухового проходу. Матеріалом для дослідження слугували поперечні зрізи внутрішньочерепної (цистернальної) частини лицевого нерва, отримані від 96 трупів людських обох статей на різних етапах постнатального розвитку. Згідно з анамнезом, у жодному випадку не було виявлено патологічних змін в області черепа або скроневої кістки, а також не було зафіксовано патологій самого лицьового нерва. Для гістологічного дослідження трупи було поділено п'ять вікових груп: I група (7–12 років) – 8 трупів; II група (13–20 років) – 11 трупів; III група (21–35 років) – 22 трупи; IV група (36–57 років) – 35 трупів; V група (58–74 років) – 20 трупів. Зразки фіксували у розчині, що містить 2 % параформальдегіду, 2 % глутарового альдегіду та 0,1 % пікринової кислоти на основі 0,1М фосфатного буфера (pH 7,4). Результати показали, що в дорослих осіб лицьовий нерв або овальної, або нечітко окресленої форми, проте його конфігурація немає прямого зв'язку з внутрішньої організацією нерва. Кількість та розташування нервових пучків, а також їх мієлоархітектонічна будова визначаються особливостями раннього онтогенезу. Також встановлено, що форма, розміри, число та топографія нервових пучків є змінними параметрами, що залежать від індивідуальних особливостей, так і від віку. Ці показники тісно пов'язані з будовою сполучнотканинної строми нервового стовбура.

Ключові слова: лицевий нерв, мієлоархітектоніка, мієлінові нервові волокна, сполучнотканинна строма.

A review of the literature shows that the study of the intratemporal structure of the facial nerve has been a focus of researchers' attention for many years [3]. The majority of studies have been dedicated to the extracranial segment of the nerve – specifically, the part following its exit from the stylomastoid foramen. This focus is of particular importance for addressing the complications that arise during the restoration of the nerve after injuries sustained in surgical interventions in the middle ear, parotid gland, and the cervicofacial region. The individual variability of each peripheral nerve is reflected in changes in the number and spectrum of myelinated fibers at different stages of life. In the dynamics of the formation of the intratemporal structure of the facial nerve, three main developmental stages are distinguished: active

development and differentiation of myelinated nerve fibers and connective tissue; a period in which the main parameters of the nerve remain relatively stable; and involutional shifts and destabilization of the conductive and stromal elements [5]. It should be noted that the limited number of studies on the internal structure of the facial nerve have primarily focused on its segment located within the temporal bone [4, 11]. These studies are particularly significant in the context of evaluating structural changes in the nerve during intracanalar inflammation or compression – factors considered relevant in the etiopathogenesis of idiopathic palsies such as Bell's palsy. The morphometric characteristics of the facial canal and their potential compressive effect on the nerve are of special interest in this regard. It has been observed that there are only a limited number of studies concerning the myeloarchitectonics of the facial nerve, particularly its intracranial – cisternal segment [7, 13].

The purpose of the study was to investigate the age-related morphological characteristics of the segment of the facial nerve extending from the brainstem to the internal acoustic meatus.

Materials and methods. The research material was obtained from the intracranial segments of the facial nerve of 96 cadavers, collected between 2020 and 2024 from the morgues of the Forensic Medical Examination and Pathological Anatomy Union – a public legal entity under the Ministry of Health of the Republic of Azerbaijan. For histological examination, the cadavers from which the study material was obtained were divided into five age groups: group I (7–12 years) – 8 cadavers; group II (13–20 years) – 11 cadavers, group III (21–35 years) – 22 cadavers, group IV (36–57 years) – 35 cadavers and group V (58–74 years) – 20 cadavers. The number of tissue sections obtained for each age group is presented in Fig. 1.

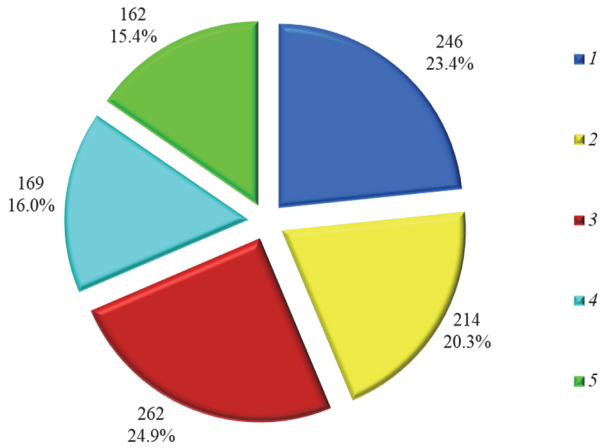

Fig. 1. Distribution of sections taken from the intracranial segment of the facial nerve for histological examination by age groups. 1, 2, 3, 4, 5 – age groups.

Samples were fixed in a solution consisting of 2 % paraformaldehyde, 2 % glutaraldehyde, and 0.1 % picric acid prepared in 0.1 M phosphate buffer (pH 7.4). After remaining in the fixative for at least 24 hours, the samples were post-fixed for two hours in a 1 % osmium tetroxide solution, also prepared in phosphate buffer (pH 7.4). Araldite-Epon blocks were prepared from the material according to standard electron microscopy protocols . Semi-thin sections (1–2 μm) were obtained using a Leica EM UC7 ultramicrotome, stained with methylene blue, azure II and basic fuchsin, or toluidine blue, and examined under a Primo Star (Zeiss) light microscope. Relevant regions were photographed using a Canon EOS D650 digital camera. Ultra-thin sections (50–70 nm) cut from the same blocks were stained first with 2 % uranyl acetate and then with 0.6 % lead citrate prepared in 0.1N NaOH. These sections were examined using a JEM-1400 transmission electron microscope operated at 80–120 kV, and electron micrographs were taken. For each section, the area and perimeter of the nerve bundle and its fragments were measured, as well as the shape factor coefficient, which characterizes the morphology of the nerve fibers within the bundle.

Quantitative data obtained during the study were analyzed using IBM SPSS Statistics version 26, employing methods of variation and dispersion analysis. Descriptive statistics for the variation series included the mean (M), standard error (±m), 95 % confidence interval (95 % CI), and central tendency measures such as the median (Me), quartiles (Q1, Q3), minimum, and maximum values. Analysis of variance (ANOVA) was applied for preliminary comparison of the data series. Differences between grouped variables were assessed using the F-test (Fisher's criterion). In comparisons involving two groups, results were further clarified using the non-parametric Mann–Whitney U test. The null hypothesis was rejected when the difference was statistically significant at $p < 0.050$. Additionally, for each age group, the frequency of occurrence of specific parameters relative to the group mean was determined.

Results of the study and their discussion. In the sections examined, the facial nerve predominantly exhibited an oval or irregular configuration. It should be noted that these morphological shape variations are not directly related to the internal structural characteristics of the nerve.

Furthermore, the number of nerve bundles, their conductive properties, and the myeloarchitectonics of the nerve are predetermined by the characteristics of early ontogenesis. Studies

have shown that the shape, size, number, and topography of the nerve bundles are variable parameters. These indicators are influenced by individual anatomical features and age-related changes and are closely associated with the connective tissue stroma of the nerve trunk (Fig. 2).

The facial nerve typically consists of several nerve fascicles. The configuration of these fascicles can vary even within the same nerve trunk, and their sizes exhibit a wide range of variation. Usually, 2–3 large fascicles are located in the central part of the nerve trunk, while smaller fascicles are observed in the peripheral regions. These smaller fascicles generally consist of dozens of myelinated nerve fibers, which are densely packed. This dense arrangement is associated with the underdevelopment of the endoneurium. In some cases, the fascicles are distributed unevenly. A structural pattern has been identified: the smaller the size of individual fascicles, the greater their number, and vice versa.

In certain cases, the nerve is composed of a small number of large fascicles that are morphologically similar to one another. Analysis of the cisternal (intracranial) segment of the nerve trunk revealed the absence of both the perineurium and epineurium.

In the adult age period, the number of nerve fascicles does not change, and there are no significant alterations in the connective tissue sheaths. The obtained results suggest that adulthood can be considered a stage during which all parameters of the facial nerve remain stable. Nevertheless, by the end of adulthood, a decrease in the total area of conductive elements and a relative increase in connective tissue stroma are observed (Fig. 3).

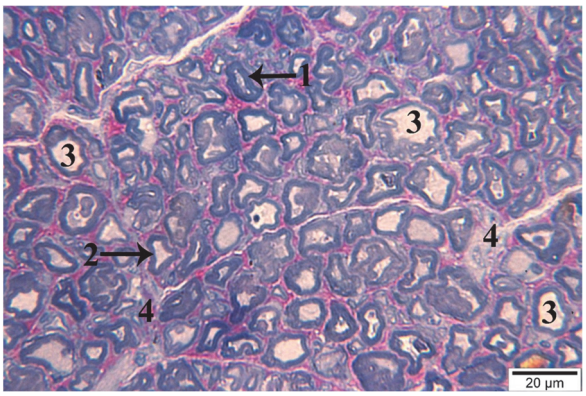

Fig. 2. Structure of an ultrathin light microscopy section of the left cisternal segment of the facial nerve obtained from a 21-year-old cadaver. 1 – myelinated nerve fiber; 2 – myelin sheath; 3 – axon; 4 – endoneurial sheath.

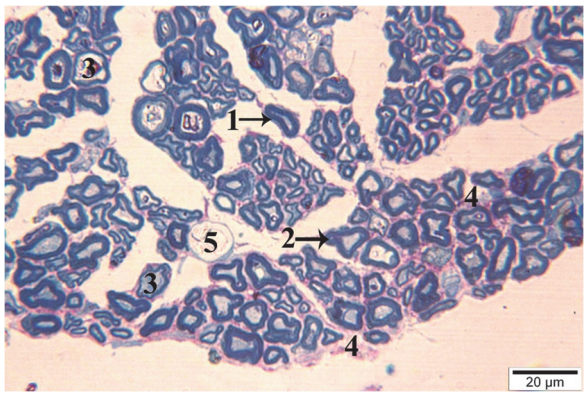

Fig. 3. Structure of an ultrathin light microscopy section of the left cisternal segment of the facial nerve obtained from a 58-year-old cadaver. 1 – myelinated nerve fiber; 2 – myelin sheath; 3 – axon; 4 – endoneurial sheath.

These findings indicate that the processes of myelination and differentiation of myelinated nerve fibers are mostly completed during adulthood. In age group I, the area of the main nerve fascicle was 5.797.741.09 µm², and its fragment measured 21.132.53 µm². The perimeter of the main fascicle was 11.305.06 µm, while that of the fragment was 597.27 µm. The shape factor was 0.57 for the main fascicle and 0.75 for the fragment.

The number of myelinated fibers in the fascicle was 67.490, occupying a total area of 14,648.27 µm², which constitutes 69.32 % of the total fascicle area. The average diameter of small myelinated fibers was 2.64±0.07 µm (min–max: 1.63–3.95 µm), medium fibers – 6.06±0.13 µm (4.03–7.98 µm), and large fibers – 9.57±0.12 µm (8.01–11.84 µm). Small-diameter fibers made up 32.5 % (21,934 fibers), medium-diameter fibers – 34.6 % (23352 fibers), and large-diameter fibers – 32.9 % (22204 fibers), indicating an approximately equal distribution.

In age group II, the main fascicle area was 511.090.46 µm², the perimeter – 3.426.64 µm, and shape factor – 0.57. The fragment measured 18.534.24 µm² in area, 545.43 µm in perimeter, and had a shape factor of 0.78.

The area occupied by myelinated fibers was 9,573.21 µm², accounting for 51.65 % of the fascicle. A total of 5,901 myelinated fibers were observed. Among them, fibers of 1–4 µm comprised 23.36 % (1,379 fibers), 4–8 µm – 50.47 % (2978 fibers), and 8–12 µm – 26.17 % (1545 fibers).

The mean diameters were: 3.24±0.083 µm (1.92–3.99 µm) for 1–4 µm fibers, 5.82±0.11 µm (4.01–7.89 µm) for 4–8 µm fibers, and 9.48±0.13 µm (8.02–11.71 µm) for 8–12 µm fibers.

In age group III, the main fascicle area was 4,075,541.78 µm², perimeter – 8,740.43 µm, and shape factor – 0.67. The fragment had an area of 21.132.53 µm², perimeter – 593.27 µm, and shape factor – 0.75. The area of myelinated fibers was 16,290.91 µm², which made up 77.08 % of the fascicle. A total of 50,528 myelinated fibers were counted. The average diameter of 1–4 µm fibers was 3.05±0.07 µm (1.73–3.99 µm),

4–8 μm – 6.20±0.12 μm (4.07–7.98 μm), and 8–12 μm – 9.11±0.07 μm (8.01–11.55 μm). Fiber distribution: 22.52 % (11,379 fibers) for 1–4 μm, 41.22 % (20,828 fibers) for 4–8 μm, and 36.26 % (18,321 fibers) for 8–12 μm.

In age group IV, the main fascicle area was 4.961.667.56 μm², perimeter – 9.469.64 μm, and shape factor – 0.70. The fragment had an area of 21.114.17 μm², perimeter – 593.15 μm, and shape factor – 0.75. Myelinated fibers occupied 17.298.42 μm², comprising 81.93 % of the fascicle. The total number of myelinated fibers was 39,714. Of these, 21.3 % (8,459 fibers) were 1–4 μm, 32.54 % (12,923 fibers) were 4–8 μm, and 46.16 % (18,332 fibers) were 8–12 μm. The mean diameters were: 2.99±0.10 μm (1.94–3.98 μm) for small, 6.22±0.16 μm (4.05–7.86 μm) for medium, and 9.66±0.11 μm (8.08–11.49 μm) for large fibers.

In age group V, the main fascicle area was 4,929,089.96 μm², perimeter – 9,452.50 μm, and shape factor – 0.69. The fragment area was 21.132.53 μm², perimeter – 593.27 μm, and shape factor – 0.75. During the examination, the area occupied by myelinated nerve fibers was 15,764.90 μm², accounting for 74.6 % of the fascicle. A total of 37,786 myelinated nerve fibers were identified within the fascicle. Among them, fibers with a diameter of 1–4 μm constituted 16.69 % (6,306 fibers), those with a diameter of 4–8 μm – 40.73 % (15,390 fibers), and fibers with a diameter of 8–12 μm – 42.58 % (16,090 fibers). We also determined that in this age group, the average diameter of small-caliber fibers was 3.08±0.09 μm (min–max: 2.4–3.94 μm), medium-caliber fibers – 6.09±0.15 μm (min–max: 4.03–7.99 μm), and large-caliber fibers – 9.63±0.12 μm (min–max: 8.01–11.76 μm).

After determining the mean values of the diameter, perimeter, area, and shape factor of myelinated fibers by age groups, as well as assessing the intra- and intergroup statistical significance of differences, we analyzed the frequency distribution of each parameter around its mean values.

Statistical analysis of the frequency distribution of myelinated fiber diameters across age groups revealed that in Group I, the most frequent diameters were within the ranges of 2.0–4.0 μm and 8.0–10.0 μm. In contrast, the frequency of fibers within the 4.0–8.0 μm range was comparatively lower in group A (Fig. 4A).

In Group II, the distribution of fiber diameters between 2.0 μm and 10.0 μm was relatively homogeneous, with fibers of different calibers occurring at comparable frequencies. A similar trend was observed in Group III. However, in this age group, the histogram exhibited a right-skewed pattern, indicating a higher frequency of larger-diameter myelinated fibers.

This indicates that as age increases, the number and frequency of occurrence of large-diameter myelinated nerve fibers also increase. In the IV and V age groups, the distribution of diameter values appears more balanced and stable. The frequent observation of myelinated fibers within the 2.0–12.0 μm range at these stages suggests that the diametric parameters tend to expand and appear more frequently with advancing age.

Fig. 4B presents the frequency analysis of the perimeters of myelinated fibers. It reveals that in the I–III age groups, the frequency of perimeter values is below the average level, whereas in the IV and V age groups, fibers with larger perimeters are observed more frequently.

According to the analysis in Fig. 4C, in the I–III age groups, myelinated fibers with a surface area greater than 100 μm² are observed at a relatively high frequency. However, the frequency of fibers with smaller surface areas particularly in the I age group – is notably low, especially at minimal values. In contrast, in the IV and V age groups, surface area values are concentrated around the mean, and the frequency distribution appears more uniform and stable. This demonstrates that with aging, the variation in the surface area of myelinated fibers decreases, and the morphometric parameters shift toward a more stabilized structural profile.

A group of authors [12] note that the true fascicular organization of the facial nerve forms after the geniculate ganglion. In their study of 60 cross-sections of facial nerves taken from 30 embalmed adult cadavers, they report that the intranuclear structure of the facial nerve is not yet fully developed proximal to the geniculate ganglion; perineurium and epineurium are absent in the pontine-cerebellar cistern. Overall, the researchers emphasize that the number of nerve fibers in the facial nerve increases from proximal to distal segments.

It is also noted that the perineurium and endoneurium are not observed in the cisternal and internal auditory canal segments of the facial nerve. Our results fully coincide with this view. We consider that the brain's pia mater envelops the nerve, forming its external connective tissue sheath.

In our previous study [6], we conducted a detailed investigation of the myeloarchitecture and age-related characteristics of the extracranial trunk of the facial nerve. We would like to present some fragments of the obtained results.

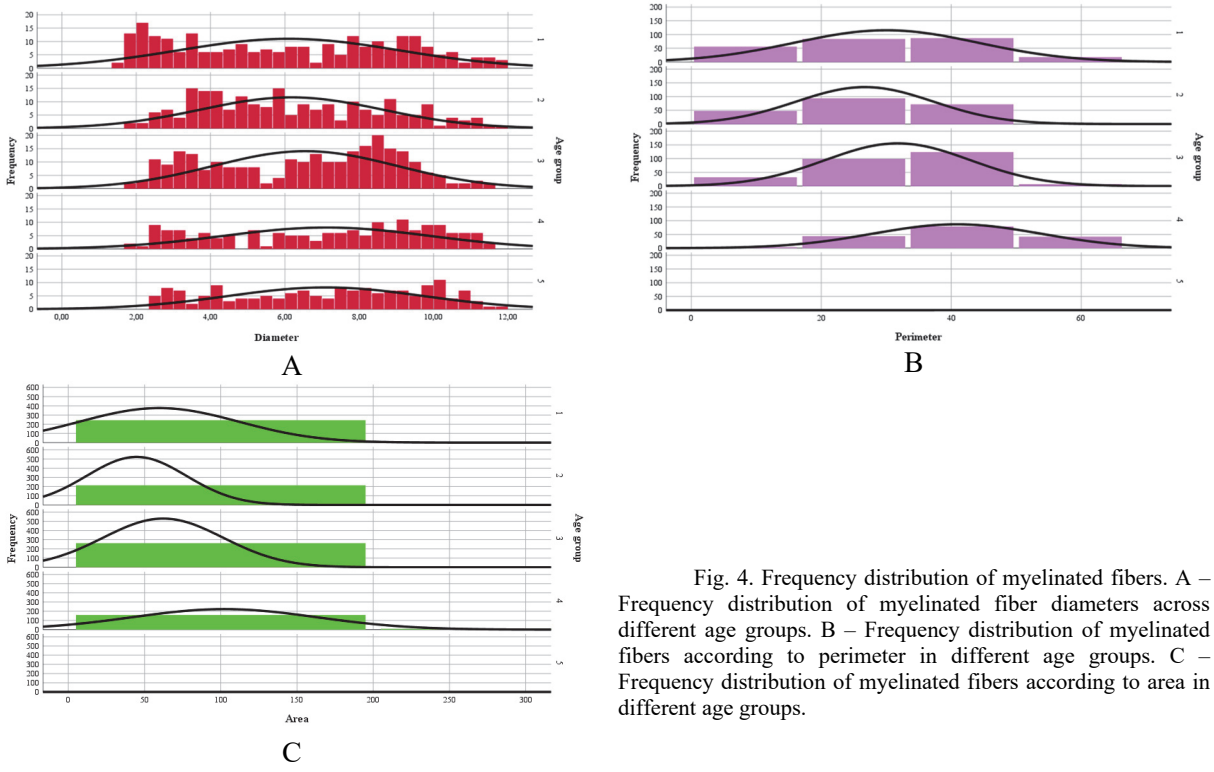

Fig. 4. Frequency distribution of myelinated fibers. A – Frequency distribution of myelinated fiber diameters across different age groups. B – Frequency distribution of myelinated fibers according to perimeter in different age groups. C – Frequency distribution of myelinated fibers according to area in different age groups.

The study showed that in adults, the diameter of the facial nerve ranges from 1697.4±51.1 μm on the right side to 1630.4±56.1 μm on the left side. This parameter is quite stable and does not show significant changes during adulthood. At the section level, the shape of the nerve is oval or irregular, but its configuration is not directly related to the internal structure of the nerve.

The results of our studies are consistent with the data on individual and age-related variability of the facial nerve [10]. In this respect, the changes observed in the facial nerve do not fundamentally differ from similar processes occurring in other structures of the nervous system.

Considering the morphological changes observed in nerves studied during old age, it should be noted that these changes affect both the conductive elements of the nerve and the connective tissue stroma. The total number of myelinated fibers decreases, the myelin sheath becomes thinner, and loses its tintorial characteristics. The obtained results correspond to materials presented in studies related to other peripheral nerves [8, 9].

Engelmann S. and colleagues [2] estimated the total number of axons in the extracranial trunk of the facial nerve to be 6684±1884, while Hembd A. et al. [8] assessed it as 5329±1376.

The intracanalicular structure of the trunk in the facial canal has been studied in more detail by representatives of Kharkiv National Medical University. Using complex morphological methods – macroscopy, histotopography, and microscopy – Lupir M. investigated the intracanalicular structure of the facial nerve in fetal, newborn, and adult human cadavers in different sections of the canal. The author reports that the average number of myelinated fibers was 8458.5±976.4 in the internal auditory canal, 10723±993.2 inside the canal, and 8720.4±887.6 slightly below the stylomastoid foramen. Analysis of the composition of myelinated fibers of various sizes at the level of the internal auditory canal showed a predominance of medium-diameter fibers (10–73 %) and large-diameter fibers (20–80 %). Proximally from the geniculate ganglion, the composition of myelinated fibers changes slightly – large-diameter fibers constitute 15–70 %, medium-diameter fibers 20–60 %, and small-diameter fibers 10–35 % [1].

Conclusion

Thus, as a result of our study, it was determined that epineurium and perineurium are not observed in the cisternal segment of the facial nerve. The ultrastructural organization of the nerve trunk and nerve fragment revealed age-related differences in the frequency distribution of myelinated nerve fibers' diameter, perimeter, area, and shape. These differences mainly increase from ages 7–12 and decrease in old age. The obtained results can be used in creating the myeloarchitecture of the facial nerve – that is, its morphological and functional mapping – and in identifying functional pathways corresponding to different axon populations.

Thus, ultrastructural analysis of the cisternal segment of the facial nerve showed that age-related changes in the nerve are closely related not only to changes in the connective tissue, but also to changes in the quantitative and qualitative parameters of its myelinated fibers. This natural "model" can also be used as an important basis for explaining ontogenetic changes observed in other peripheral nerves.

References

1. Lupyr MV. Strukturna orhanizatsiia lytsevoho nerva v kanali vysonochnoyi kistky. Aktualni problemy suchasnoyi medytsyny. 2013;13(4):128–132. [in Ukrainian].
2. Engelmann S, Ruewe M, Geis S. Rapid and Precise Semi-Automatic Axon Quantification in Human Peripheral Nerves [published correction appears in Sci Rep. 2020 Apr 17;10(1):6865]. https://doi.org/10.1038/s41598-020-58917-4.
3. Guttal C, Prasad K, Kv V, G I, S G. Revisiting the Intratemporal Course of the Facial Nerve. Cureus. 2024 Nov 8;16(11):e73280. https://doi.org/10.7759/cureus.73280.
4. Haginomori S. Histological anatomy of the human temporal bone for ear surgery. Jibi Inkokka Tembo. 2021;64(5):268–277. https://doi.org/10.11453/orltokyo.64.5_268.
5. Hembd A, Nagarkar P, Perez J. Correlation between Facial Nerve Axonal Load and Age and Its Relevance to Facial Reanimation. Plast Reconstr Surg. 2017;139(6):1459-1464. https://doi.org/10.1097/PRS.0000000000003376.
6. Kerimzade G, Movsumov N, Shadlinskaya S. Features of Structural Organization of the Human Facial Nerve. Journal of Islamic International Medical College. 2024; (4):267–271. https://journals.riphah.edu.pk/index.php/jiimc/article/view/2194.
7. Kochhar A, Larian B, Azizzadeh B. Facial Nerve and Parotid Gland Anatomy. Otolaryngol Clin North Am. 2016;49(2):273-284. https://doi.org/10.1016/j.otc.2015.10.002.
8. Mohanty AJ, van Rooij JAF, Misere RML, Lataster A, Rozen SM, van Der Hulst RRWJ, et al. Anatomy and Histology of Sensorimotor Connections Between the Facial and Trigeminal Nerve in the Buccinator Muscle. Head and Neck. 2025 Mar;47(3):928–935. https://doi.org/10.1002/hed.27990.
9. Ozgen Mocan B. Imaging Anatomy and Pathology of the Intracranial and Intratemporal Facial Nerve. Neuroimaging Clin N Am. 2021;31(4):553–570. doi:10.1016/j.nic.2021.06.001.
10. Seneviratne SO, Patel BC. Facial Nerve Anatomy and Clinical Applications. In: StatPearls [Internet]. Treasure Island (FL): StatPearls Publishing; 2025 Jan–. Available from: https://www.ncbi.nlm.nih.gov/books/NBK554569/.
11. Talas DÜ, Beger O, Koç T, Hamzaoğlu V, Özalp H, Mavruk M, et al. Morphometric properties of the facial nerve in fetal temporal bones. Int J Pediatr Otorhinolaryngol. 2019;116:7–14. https://10.1016/j.ijporl.2018.10.012.
12. Yang SH, Park HK, Yoo DS, Joo W, Rhoton A. Microsurgical anatomy of the facial nerve. Clin Anat. 2021;34(1):90–102. https://doi.org/10.1002/ca.23652.
13. Yee Gi-T, Yoo Ch-J, Han S-R, Choi Ch-Y. Microanatomy and histological features of central myelin in the root exit zone of facial nerve. J Korean Neurosurg Soc. 2014 May;55(5):244–247. doi: 10.3340/jkns.2014.55.5.244.

Стаття надійшла 26.07.2024 р.